Medial axis lookup table and test neighborhood computation for 3D chamfer norms

Nicolas Normand[*], Pierre Evenou

IRCCyN UMR CNRS 6597, École polytechnique de l'Université de Nantes, Rue Christian Pauc, La Chantrerie, 44306 Nantes Cedex 3, France

ABSTRACT

Chamfer distances are discrete distances based on the propagation of local distances, or weights, defined in a mask. The medial axis, i.e. the centers of maximal balls (balls which are not contained in any other ball), is a powerful tool for shape representation and analysis. The extraction of maximal disks is performed in the general case by testing the inclusion of a ball in a local neighborhood with covering relations usually represented by lookup tables.

The proposed method determines if a mask induces a norm and in this case, computes the lookup tables and the test neighborhood based on geometric properties of the balls of chamfer norms, represented as $\mathcal{H}$-polytopes. The method does not need to repeatedly scan the image space, and improves the computation time of both the test neighborhood detection and the lookup table computation.

© 2008 Elsevier Ltd. All rights reserved.

1. Introduction

The distance transform DT_X of a binary image X is a function that maps each point p to its distance to the closest background pixel i.e. with the radius of the largest open disk centered in p included in the image. Such a disk is said to be maximal if it is not contained in another disk also included in X. The set of centers of maximal disks, also called the medial axis, is a convenient description of binary images for many applications ranging from image coding to shape recognition. Its attractive properties are reversibility and (relative) compactness.

Algorithms for computing the distance transform are known for various discrete distances [1–5]. In this paper, we will focus on chamfer (or weighted) distances which are defined by a set of weighted vectors described by a mask, called the *chamfer mask*. The classical medial axis extraction method is based on the removal of non-maximal disks in the distance transform. It is thus mandatory to describe the covering relation of disks, or at least the transitive reduction of this relation. For simple distances, this knowledge is summarized in a local maximum criterion [1] but a most general method uses lookup tables (LUT) for that purpose [6].

In this paper, we propose a two-phase method that determines if a mask induces a norm and in this case, computes the LUT and the test neighborhood based on geometric properties of the balls of chamfer norms.

The first phase starts from the 3D chamfer mask and produces a triangulation of the chamfer neighbors inversely pondered by the chamfer weights. The algorithm conceptually operates on the convex hull of these weighted vectors and creates a triangulation of this convex hull. It produces two results: a norm condition check and a description of the geometry of the chamfer balls for the given chamfer mask. The second phase is performed only for norms; from the general geometry obtained during the previous phase, each chamfer ball is described as the intersection of a set of half-spaces ($\mathcal{H}$-description). The norm condition is sufficient for the balls to be convex, ensuring the validity of their $\mathcal{H}$-description. This $\mathcal{H}$-description is then used to compute the test neighborhood $\mathcal{T}$ and the LUT values.

Basic notions, definitions and known results about chamfer disks and medial axis LUT are recalled in Section 2. Then Section 3 justifies the use of polytope formalism in our context and presents the principles of the method. In Section 4, a triangulation algorithm is given for the 3D case. The computation of the test neighborhood $\mathcal{T}$ and of the LUT values is explained in Section 5. Finally, Section 6 gives speed-up figures for the overall algorithm compared to a reference implementation [7]. Notice that we do not address the actual computation of the medial axis which remains unchanged.

This paper is a more detailed version of [8] with an added method for the triangulation of 3D balls and the detection of norm conditions. The algorithms for LUT and $\mathcal{T}$ computation were adapted to the 3D case from [8].

* Corresponding author. Tel.: +33 2 40 68 32 07; fax: +33 2 40 68 32 32.
  E-mail addresses: Nicolas.Normand@polytech.univ-nantes.fr (N. Normand),
Pierre.Evenou@polytech.univ-nantes.fr (P. Evenou).

2. Chamfer distances and medial axis

2.1. Discrete distances

Definition 1 (*Discrete distance, metric and norm*). Consider a function $d : \mathbb{Z}^n \times \mathbb{Z}^n \to \mathbb{N}$ and the following properties $\forall x, y, z \in \mathbb{Z}^n$, $\forall \lambda \in \mathbb{Z}$:

1. *positive definiteness* $d(x, y) \geqslant 0$ and $d(x, y) = 0 \Leftrightarrow x = y$,
2. *symmetry* $d(x, y) = d(y, x)$,
3. *triangle inequality* $d(x, z) \leqslant d(x, y) + d(y, z)$,
4. *translation invariance* $d(x + z, y + z) = d(x, y)$,
5. *positive homogeneity* $d(\lambda x, \lambda y) = |\lambda| \cdot d(x, y)$.

d is called a *distance* if it verifies conditions 1 and 2, a *metric* with conditions 1–3 and induces a *norm* if it also satisfies conditions 4 and 5.

Most discrete distances are built from a definition of neighborhood and connected paths (path-based distances), the distance between two points being equal to the length of the shortest path that joins them [9]. Distance functions differ by the neighborhoods used to build paths and by the way path lengths are measured. For the simple distance d_4 (denoted by d in [1]), defined in the square grid $\mathbb{Z}^2$, each pixel has four neighbors located at its top, left, bottom and right edges. Similarly, for distance d_8 (d^* in [1]), each pixel has four extra diagonally located neighbors. In both cases, d_4 and d_8, the length of a path is defined as its number of displacements, whereas it is measured as a weighted sum of displacements for chamfer distances [2,3] or by the displacements allowed at each step for neighborhood sequence distances [3,9], or even by a mixed approach of weighted neighborhood sequence paths [5].

For a given distance d, the closed ball $B_\leqslant$ and open ball $B_<$ of center c and radius r are the sets of points of $\mathbb{Z}^n$:

$$B_<(c, r) = \{p : d(c, p) < r\},$$

$$B_\leqslant(c, r) = \{p : d(c, p) \leqslant r\}. \qquad (1)$$

Since the codomain of d is $\mathbb{N}$, we have $\forall r \in \mathbb{N}$, $d(c, p) \leqslant r \Leftrightarrow d(c, p) < r + 1$. So

$$\forall r \in \mathbb{N}, \quad B_\leqslant(c, r) = B_<(c, r + 1). \qquad (2)$$

Definition 2 (*Distance transform*). The distance transform DT_X of the binary image X is a function that maps each point p to its distance to the closest background pixel:

$$DT_X : \mathbb{Z}^n \to \mathbb{N},$$

$$DT_X(p) = \min\{d(p, q) : q \in \mathbb{Z}^n \backslash X\}. \qquad (3)$$

Alternatively, since all points at a distance less than $DT_X(p)$ from p belongs to X ($B_<(p, DT_X(p)) \subset X$) and at least one point at a distance equal to $DT_X(p)$ is not in X ($B_\leqslant(p, DT_X(p)) = B_<(p, DT_X + 1) \not\subset X$) then $DT_X(p)$ is the radius of the largest open disk centered in p included in the image:

$$DT_X(p) = \max\{r : B_<(p, r) \subset X\}. \qquad (4)$$

Definition 3 (*Medial axis*). The medial axis MA_X of the binary image X is the set of centers of maximal open balls in X valued with their radii:

$$MA_X : \mathbb{Z}^n \to \mathbb{N},$$

$$MA_X(p) = \begin{cases} 0 & \text{if } \exists q, r' \text{ s.t. } B_<(p, DT_X(p)) \subsetneq B_<(q, r') \subset X, \\ DT_X(p) & \text{otherwise.} \end{cases} \qquad (5)$$

2.2. Chamfer distances

Definition 4 (*Chamfer mask, Thiel [10]*). A weighting $M = (\vec{v} ; w)$ is a vector $\vec{v}$ of $\mathbb{Z}^n$ associated with a weight w (or local distance). A chamfer mask $\mathscr{M}$ is a central-symmetric set of weightings having positive weights and non-null displacements, and containing at least one basis of $\mathbb{Z}^n$: $\mathscr{M} = \{M_i \in \mathbb{Z}^n \times \mathbb{N}^*\}_{1 \leqslant i \leqslant m}$.

The grid $\mathbb{Z}^n$ is symmetric with respect to the hyperplanes normal to the axes and to the bisectors (G-symmetry). This divides $\mathbb{Z}^n$ into $2^n.n!$ subspaces (there are eight of them for $\mathbb{Z}^2$ and 48 for $\mathbb{Z}^3$). The particular subspace $x_n \geqslant \cdots \geqslant x_1 \geqslant 0$ is called the generator cone or simply generator and is denoted $\mathscr{G}$. From every point in $\mathbb{Z}^n$, we can determine its unique G-symmetrical point in $\mathscr{G}$ by ordering the absolute values of its components in decreasing order. Conversely, from any point p in $\mathscr{G}$, we can derive all its G-symmetrical points by generating all $n_1!$ permutations of the components of p and all 2^{n_2} combinations of their signs where n_1 and n_2 are, respectively, the number of different absolute values of the components of p and the number of non-null components.

Chamfer masks are usually restricted to $\mathscr{G}$ for simplicity. Weightings are then only given in $\mathscr{G}$ and we denote $\mathscr{M}|_\mathscr{G} = \{M_i \in \mathscr{G} \times \mathbb{N}^*\}_{1 \leqslant i \leqslant m}$, the chamfer mask restricted to $\mathscr{G}$. A usual ordering of the points in $\mathscr{G}$ is the lexicographical order; p is before q if for some i: $p_{0...i-1} = q_{0...i-1}$ and $p_i < q_i$. According to this ordering, a common naming scheme assigns alphabetic letters to visible points (such that $\gcd(p) = 1$). For instance, in the 2D grid: $\vec{a} = (1 \ 0)$, $\vec{b} = (1 \ 1)$, $\vec{c} = (2 \ 1)$, $\vec{d} = (3 \ 1)$, $\vec{e} = (3 \ 2) \ldots$. The corresponding chamfer weights are, respectively, named $a, b, c, d, e \ldots$.

Definition 5 (*Chamfer distance, Thiel [10]*). Consider the chamfer mask $\mathscr{M} = \{(\vec{v_i} ; w_i) \in \mathbb{Z}^n \times \mathbb{N}^*\}_{1 \leqslant i \leqslant m}$. The chamfer (or weighted) distance between two points p and q is

$$d(p, q) = \min \left\{ \sum \lambda_i w_i : p + \sum \lambda_i \vec{v_i} = q, \lambda_i \in \mathbb{N}, 1 \leqslant i \leqslant m \right\}. \qquad (6)$$

Paths between two points p and q can be produced by chaining displacements. The length of a path is the sum of the weights associated with the displacements and the distance between p and q is the length of the shortest path.

Any chamfer masks defines a metric [11]. However, a chamfer mask only generates a norm when proper conditions on the mask neighbors and on the corresponding weights permits a triangulation of the ball in influence cones [10,12]. When a mask induces a norm then all its balls are convex and therefore can be represented as polytopes.

2.3. Chamfer medial axis

For simple distances d_4 and d_8, the medial axis extraction can be performed by the detection of local maxima in the distance map [1]. Chamfer distances raise a first complication even for small masks as soon as the weights are not unitary. Since all possible values of distance are not achievable, two different radii r and r' may correspond to the same set of discrete points. The radii r and r' are said to be *equivalent*. Since the distance transform labels pixels with the greatest equivalent radius, criteria based on radius difference fail to recognize equivalent disks as being covered by other disks. In the case of 3×3 2D masks or $3 \times 3 \times 3$ 3D masks, a simple relabeling of distance map values with the smallest equivalent radius is sufficient [13,14]. However, this method fails for greater masks and the most general method for medial axis extraction from the distance map involves LUT that represent for each neighbor $\vec{v_i}$ in a set called the test neighborhood $\mathscr{T}$ and for each radius r_1, the minimal open

a

$$\mathscr{T} = \left\{ \vec{a} = (1\ 0); \vec{b} = (1\ 1); \vec{c} = (2\ 1) \right\}$$

b

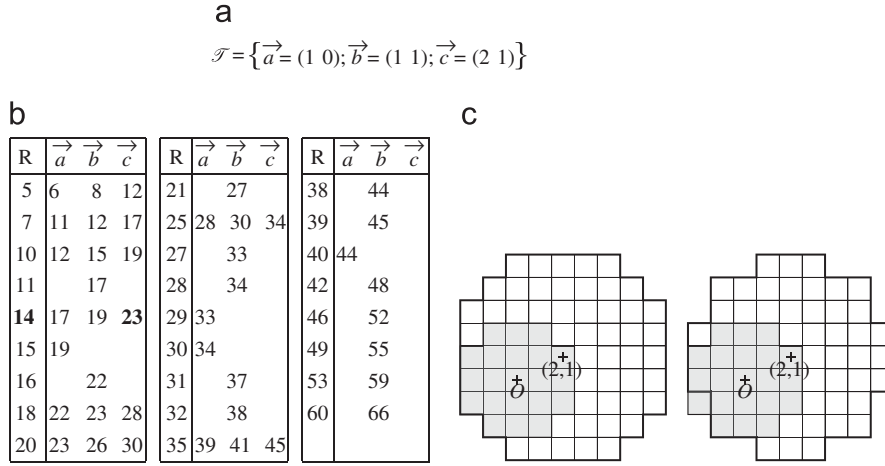| R	$\vec{a}$	$\vec{b}$	$\vec{c}$	R	$\vec{a}$	$\vec{b}$	$\vec{c}$	R	$\vec{a}$	$\vec{b}$	$\vec{c}$
5	6	8	12	21		27		38		44	
7	11	12	17	25	28	30	34	39		45	
10	12	15	19	27		33		40	44		
11		17		28		34		42		48	
14	17	19	**23**	29	33			46		52	
15	19			30	34			49		55	
16		22		31		37		53		59	
18	22	23	28	32		38		60		66	
20	23	26	30	35	39	41	45				

c

Fig. 1. (a) Test neighborhood and (b) lookup table for distance $d_{5,7,11}$ extracted from [7, Fig. 14]. The value $\text{Lut}_{\vec{c}}(14) = 23$ (in boldface) means that $B_<(O, 14) \subseteq B_<(O + \vec{c}, 23)$ as shown in (c) but $B_<(O, 14) \nsubseteq B_<(O + \vec{c}, 22)$ because of the point $(-2, 1)$ (d). In terms of closed balls, $B_\leqslant(O, 13) \subseteq B_\leqslant(O + \vec{c}, 22)$ but $B_\leqslant(O, 13) \nsubseteq B_\leqslant(O + \vec{c}, 21)$.

ball covering $B_<(O, r_1,)$ in direction $\vec{v_i}$ [6]:

$$\text{Lut}_{\vec{v_i}}(r_1) = \min\{r_2 : B_<(O + \vec{v_i}, r_1) \subseteq B_<(O, r_2)\}.$$

Equivalently, using closed balls (considering (2)):

$$\text{Lut}_{\vec{v_i}}(r_1) = 1 + \min\{r_2 : B_\leqslant(O + \vec{v_i}, r_1 - 1) \subseteq B_\leqslant(O, r_2)\}. \quad (7)$$

As noticed by Thiel, the test neighborhood $\mathscr{T}$ (Fig. 1(a)) is not necessarily equal to the chamfer mask $\mathscr{M}$ [10].

2.3.1. Medial axis LUT coefficients

A general method for LUT coefficient computation was given by Rémy and Thiel [10,15,16]. The idea is that the disk covering relation can be extracted directly from values of distance to the origin. If $d(O, p) = r_1$ and $d(O, p + \vec{v_i}) = r_2$, we can deduce the following:

$$p \in B_\leqslant(O, r_1) = B_<(O, r_1 + 1),$$
$$p + \vec{v_i} \notin B_\leqslant(O, r_2 - 1) = B_<(O, r_2),$$

hence $B_<(O + \vec{v_i}, r_1 + 1) \not\subset B_<(O, r_2)$ and $\text{Lut}_{\vec{v_i}}(r_1 + 1) > r_2$. If $\forall p, d(O, p) \leqslant r_1 \Rightarrow d(O, p + \vec{v_i}) \leqslant r_2$ then $\text{Lut}_{\vec{v_i}}(r_1 + 1) = r_2 + 1$.

Finally, $\text{Lut}_{\vec{v_i}}(r) = 1 + \max\{d(O, p + \vec{v_i}) : d(O, p) < r\}$.

This method only requires one scan of the distance function for each displacement $\vec{v_i}$. Moreover, the visited area may be restricted according to the symmetries of the chamfer mask. The order of complexity is about $O(mL^n)$ for m neighbors if we limit the computation of the distance function to an image of size L^n.

2.3.2. Medial axis test neighborhood

Thiel observed that the chamfer mask is not adequate to compute the medial axis [15, p. 81]. For instance, with $d_{14,20,31,44}$, $\text{Lut}_{(2,1)}(291) = 321$ and $\text{Lut}_{(2,1)}(321) = 352$, but the smallest open ball of center O that covers $B_<((4, 2), 291)$ is $B_<(O, 351)$. This inclusion relation is neither detected with the vector $\vec{c} = (2\ 1)$ nor with the other vectors of the chamfer mask. Remy and Thiel then introduced an LUT mask (called test neighborhood and denoted by $\mathscr{T}(R)$ here) for that purpose [12]. $\mathscr{T}(R)$ is the minimal set of vectors sufficient to detect the medial axis for shapes whose inner radius (the radius of a greatest ball) is less than or equal to R. In the previous $d_{14,20,31,44}$ example, the point $(4, 2)$ is not in the chamfer mask but should be in $\mathscr{T}(R)$ for R greater than 350.

A test neighborhood incompleteness produces extra points in the medial axis (undetected ball coverings). A general method for both detecting and validating $\mathscr{T}$ is based on the computation of the medial axis of all disks [7]. When $\mathscr{T}$ is complete, the medial axis is restricted to the center of the disk, when extra points remains, they are added to $\mathscr{T}$. This neighborhood determination was proven to work in any dimension $n \geqslant 2$. However, it is time consuming even when taking advantage of the mask symmetries.

3. $\mathscr{H}$-polytopes and chamfer balls

3.1. General $\mathscr{H}$-polytopes [17]

Definition 6 (*Polyhedron*). A convex polyhedron is the intersection of a finite set of half-hyperplanes.

Definition 7 (*Polytope*). A polytope is the convex hull of a finite set of points.

Theorem 1 (*Weyl–Minkowski*). *A subset of Euclidean space is a polytope if and only if it is a bounded convex polyhedron.*

As a result, a polytope in $\mathbb{R}^n$ can be represented either as the convex hull of its k vertices ($\mathscr{V}$-representation) or by a set of l half-planes ($\mathscr{H}$-representation):

$$P = \text{conv}(\{p_i\}_{1 \leqslant i \leqslant k}) = \left\{ p = \sum_{i=1}^{k} \alpha_i p_i : \alpha_i \in \mathbb{R}_+ \text{ and } \sum_{i=1}^{k} \alpha_i = 1 \right\}, \quad (8)$$

$$P = \{x : Ax \leqslant y\}, \quad (9)$$

where A is an $l \times n$ matrix, y a vector of n values that we name $\mathscr{H}$-coefficients of P. Given two vectors $\vec{u}$ and $\vec{v}$, we denote $\vec{u} \leqslant \vec{v}$ if and only if $\forall i, \vec{u_i} \leqslant \vec{v_i}$.

Definition 8 (*Simplicial cone*). A simplicial cone $C_{o,U}$ from a point o is a cone of dimension m defined by a set U of m independent vectors.

In a simplicial cone, each point is representable by a unique (up to a permutation) non-negative combination of the vectors of the cone, i.e.:

$$p \in C_{o,U} \Rightarrow \vec{op} = \sum_{i=1}^{m} \alpha_i \vec{u_i} \quad \text{where } (\alpha_i) \in \mathbb{R}_+^m \text{ is unique.}$$
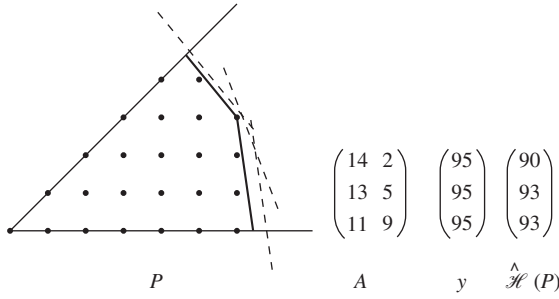
$$\begin{pmatrix} 14 & 2 \\ 13 & 5 \\ 11 & 9 \end{pmatrix} \quad \begin{pmatrix} 95 \\ 95 \\ 95 \end{pmatrix} \quad \begin{pmatrix} 90 \\ 93 \\ 93 \end{pmatrix}$$

$$P \qquad\qquad\qquad A \qquad\quad y \qquad \widehat{\mathscr{H}}(P)$$

Fig. 2. $\mathscr{H}$-representations of a discrete G-symmetrical polytope P (restricted to the first octant). Dashed lines: an $\mathscr{H}$-representation of P. Thick lines: $\widehat{\mathscr{H}}$-representation of P. In the $\widehat{\mathscr{H}}$ case, the three equalities are verified for the same point $(6, 3)$. Notice that although coefficient values are minimal, this representation is still redundant: the second inequality could be removed.

Definition 9 (*Discrete polytope*). A discrete polytope $\mathscr{Q}$ is the intersection of a polytope $\mathscr{P}$ in $\mathbb{R}^n$ with $\mathbb{Z}^n$ (Gauss discretization of $\mathscr{P}$).

Definition 10 (*Unimodular cone*). A unimodular cone $C_{o,U}$ is a simplicial cone defined by a set of integral vectors U that generate all the integral points of $C_{o,U}$.

In a unimodular cone, all discrete points are representable as a unique non-negative integral combination of the vectors of the cone. A cone $C_{o,U}$ of dimension n is unimodular if and only if $|\det(U)| = 1$. Then U is the basis of a unimodular point lattice, equivalent to $\mathbb{Z}^n$, so each integral point can be reached.

3.1.1. Minimal representation

Many operations on $\mathbb{R}^n$ polytopes in either $\mathscr{V}$ or $\mathscr{H}$ representation often require a minimal representation. The *redundancy removal* is the elimination of unnecessary points in the $\mathscr{V}$-representation or unnecessary inequalities in the $\mathscr{H}$-representation of polytopes. Since our purpose is mainly to compare $\mathscr{H}$-polytopes defined with the same matrix A, no inequality removal is needed. However, for some operations, $\mathscr{H}$-representations of discrete polytopes must be minimal in terms of $\mathscr{H}$-coefficients.

Definition 11 (*Minimal parameter representation*). A minimal parameter $\mathscr{H}$-representation of a discrete polytope P, denoted $\widehat{\mathscr{H}}$-representation, is an $\mathscr{H}$-representation of $P = \{x : Ax \leqslant y\}$ such that y is minimal:

$$P = \{x \in \mathbb{Z}^n : Ax \leqslant y\} \text{ and } \forall i \in [1 \dots l], \ \exists x \in P : A_i x = y_i, \tag{10}$$

where A_i stands for the ith line of the matrix A.

The $\widehat{\mathscr{H}}$ function, introduced for convenience, gives the minimal parameter vector for a given polytope P: $\widehat{\mathscr{H}}(P) = \max\{Ax : x \in P\}$. As a consequence, $\{x : Ax \leqslant \widehat{\mathscr{H}}(P)\}$ is the $\widehat{\mathscr{H}}$-representation of $P = \{x : Ax \leqslant y\}$. Fig. 2 depicts two representations of the same polytope P in $\mathbb{Z}^2$, one of each is minimal.

3.1.2. $\mathscr{H}$-polytope translation

Let $P = \{x : Ax \leqslant y\}$ be an $\mathscr{H}$-polytope. The translated of P by $\vec{v}$ which is also the Minkowski sum of P and $\{\vec{v}\}$ is

$$(P)_{\vec{v}} = P \oplus \{\vec{v}\} = \{x + \vec{v} : Ax \leqslant y\} = \{x : Ax \leqslant y + A\vec{v}\}. \tag{11}$$

The translation of a minimal representation gives a minimal representation.

3.1.3. Covering test

Let $P = \{x : Ax \leqslant y\}$ and $Q = \{x : Ax \leqslant z\}$ be two polyhedra represented by the same matrix A but having different sets of $\mathscr{H}$-coefficients y and z. We have

$$y \leqslant z \ \Rightarrow \ P \subseteq Q. \tag{12}$$

Furthermore, if the $\mathscr{H}$-description of the enclosed polyhedron has minimal coefficients, the condition is also necessary:

$$y = \widehat{\mathscr{H}}(P) \leqslant z \ \Leftrightarrow \ P \subseteq Q. \tag{13}$$

3.2. Geometry of the chamfer ball [10,12]

Describing balls of chamfer norms as polygons in 2D and polyhedra in higher dimensions is not new [11]. Thiel and others have extensively studied chamfer ball geometry from this point of view [12,15,18]. Our purpose is to introduce properties specific to the $\mathscr{H}$-representation of these convex balls.

We can deduce from (1) and (6) a recursive construction of chamfer balls:

$$B_{\leqslant}(O,r) = B_{\leqslant}(O, r-1) \cup \bigcup_{0 \leqslant i \leqslant m} B_{\leqslant}(O + \vec{v_i}, r - w_i). \tag{14}$$

This construction is sufficient to obtain an exact description of the balls in the case of chamfer norms as we will see later (Section 5.1).

Definition 12 (*Rational ball*). Consider a chamfer mask $\mathscr{M}$, the rational unitary ball or simply rational ball B_R is the convex hull of the rational points $\vec{v_i}/w_i$, $(\vec{v_i}, w_i) \in \mathscr{M}$:

$$B_R = \text{conv}\left(\frac{\vec{v_i}}{w_i} : (\vec{v_i}; w_i) \in \mathscr{M} \right)$$
$$= \left\{ \sum_{i=1}^{m} \alpha_i \frac{\vec{v_i}}{w_i} : \alpha_i \in \mathbb{R}_+, \sum_{i=1}^{m} \alpha_i = 1 \right\}. \tag{15}$$

Note that the rational ball, as it is introduced here, is convex by definition and is different, in this regard, from the *equivalent rational ball* described in [10,12,19].

Proposition 1. *The homothetic of B_R, rB_R contains $B_{\leqslant}(O,r)$: $B_{\leqslant}(O,r) \subseteq rB_R$.*

Proof. Let p be a point of $B_{\leqslant}(O,r)$ and $\sum_{i=1}^{m} \lambda_i \vec{v_i}$, $\lambda_i \in \mathbb{N}$ be a minimal path between O and p. Then $d(O,p) \leqslant r$ and $d(O,p) = \sum_{i=1}^{m} \lambda_i w_i$. We can describe p as a combination of O, $r\vec{v_1}/w_1, \dots, r\vec{v_n}/w_n$:

$$p = \frac{r - d(O,p)}{r} \cdot O + \sum_{i=1}^{m} \frac{\lambda_i w_i}{r} \cdot \frac{r}{w_i} \vec{v_i} \quad \text{with} \ \frac{r - d(O,p)}{r} \geqslant 0, \ \frac{\lambda_i w_i}{r} \geqslant 0 \ \forall i$$

and

$$\frac{r - d(O,p)}{r} + \sum_{i=1}^{m} \frac{\lambda_i w_i}{r} = 1.$$

Then, by definition of conv: $p \in \text{conv}(O, (r/w_1)\vec{v_1}, \dots, (r/w_n)\vec{v_n}) \subset rB_R$ and every point of $B_{\leqslant}(O,r)$ is in rB_R. $\quad\square$

Definition 13 (*Normal vector, Thiel [10]*). We call normal vector to a facet $\mathscr{F}$ of B_R, the unique vector $\vec{\mathscr{F}}$ orthogonal to the facet such that $\forall p \in \mathscr{F}$, $\vec{\mathscr{F}} \cdot p = 1$.

In the simplicial cone spanned by vectors $\vec{v_1}/w_1 \dots \vec{v_n}/w_n$, $\vec{\mathscr{F}} \cdot (\vec{v_1}/w_1 \dots \vec{v_n}/w_n) = (1 \dots 1)$. This implies

$$\vec{\mathscr{F}} = (w_1, \dots, w_n) \cdot (\vec{v_1} | \dots | \vec{v_n})^{-1}. \tag{16}$$

The vector $\alpha = (\vec{v_1}|\ldots|\vec{v_n})^{-1}p$ give the unique representation of p as a combination of $\vec{v_1}, \ldots, \vec{v_n}$. If α has integer coefficients then there is a path $\alpha(\vec{v_1}|\ldots|\vec{v_n})$ to p and its length is $(w_1, \ldots, w_n) \cdot \alpha = \vec{\mathscr{F}} \cdot p$. The normal vector is equivalent to the *elementary displacement* and *discrete gradient* of the cone intercepted by $\mathscr{F}$ as defined for chamfer norms in [10,12]. Note that the normal vector is defined here for general chamfer masks, whether they induce a norm or not.

For instance, with the chamfer norm $d_{5,7,11}$, the point $(3, 1)$ is in the cone spanned by the vectors $\vec{a} = (1\ 0)$ and $\vec{c} = (2\ 1)$ and the weights involved are 5 and 11. The distance between the origin and the point $(3, 1)$ is then [10, (4.32)]:

$$d(O, (3, 1)) = (5\ 11) \cdot \begin{pmatrix} 1 & 2 \\ 0 & 1 \end{pmatrix}^{-1} \cdot \begin{pmatrix} 3 \\ 1 \end{pmatrix} = (5\ 1) \cdot \begin{pmatrix} 3 \\ 1 \end{pmatrix} = 16.$$

3.3. Mask conditions for chamfer norms

Proposition 2 (*Distance lower bound*). *If $\mathscr{F}$ is a facet of the rational ball and $\vec{\mathscr{F}}$ its normal vector, then*:

$$d(O, p) \geqslant \vec{\mathscr{F}} \cdot p. \tag{17}$$

Proof. Let $p = \sum_i \lambda_i \vec{v_i}$ be a minimal path to p, so $d(O, p) = \sum_i \lambda_i w_i$. The facet $\mathscr{F}$ is supported by the hyperplane $\{x \in \mathbb{R}^n : \vec{\mathscr{F}} \cdot x = 1\}$. Due to convexity, the unitary ball is included in the half-space $\{x \in \mathbb{R}^n : \vec{\mathscr{F}} \cdot x \leqslant 1\}$. This applies to the vertices of the unitary ball $\vec{v_i}/w_i$: $\vec{\mathscr{F}} \cdot \vec{v_i}/w_i \leqslant 1$. By linearity of the dot product, $\vec{\mathscr{F}} \cdot \vec{v_i} \leqslant w_i$ and $\vec{\mathscr{F}} \cdot (\sum_i \lambda_i \vec{v_i}) = \sum_i \lambda_i \vec{\mathscr{F}} \cdot \vec{v_i} \leqslant \sum_i \lambda_i w_i$. Hence, $\vec{\mathscr{F}} \cdot \sum_i \lambda_i \vec{v_i}$ is always less than or equal to the length of the path $\sum_i \lambda_i \vec{v_i}$. $\square$

This lower bound applies for any point p, whether or not it is located in a cone that intercepts $\mathscr{F}$; d does not need to induce a norm.

Proposition 3 (*Homogeneity in a unimodular cone*). *Let $C_{O,U}$ be a unimodular cone that intercepts a unique facet $\mathscr{F}$ of B_R. The distance d is homogenous in the cone and equal to $\vec{\mathscr{F}} \cdot p$, $\forall p \in C_{O,U}$ if and only if*:

$$d(O, O + \vec{u}) = \vec{\mathscr{F}} \cdot \vec{u}, \quad \forall \vec{u} \in U. \tag{18}$$

Proof. According to Proposition 2, $d(O, p) \geqslant \vec{\mathscr{F}} \cdot p$, $\forall p \in C_{O,U}$. Since $C_{O,U}$ is unimodular, p is reachable by a non-negative integral combination of vectors of U, $\vec{Op} = \sum_i \lambda_i \vec{u_i}$. By triangle inequality and proposition hypotheses, $d(O, p) \leqslant \sum_i \lambda_i d(O, O + \vec{u_i}) = \sum_i \lambda_i \vec{\mathscr{F}} \cdot \vec{u_i} = \vec{\mathscr{F}} \cdot p$. So $\vec{\mathscr{F}} \cdot p$ is simultaneously a lower and upper bound to $d(O, p)$ then the equality holds and d is homogenous in $C_{O,U}$.

Conversely, consider a vector $\vec{u}$ of U such that $d(O, p) \neq p \cdot \vec{\mathscr{F}}$, so $d(O, p) > p \cdot \vec{\mathscr{F}}$, by Proposition 2. In the facet $\mathscr{F}$, we always can find $n = \dim(\mathscr{F}) + 1$ vertices $\vec{v_1}/w_1 \ldots \vec{v_n}/w_n$ such that $\vec{u}$ lies in the simplicial cone spanned by the vectors $\vec{v_1} \ldots \vec{v_n}$. As a consequence $\vec{u}$ can be represented by a unique non-negative combination of n linearly independent vectors: $\vec{u} = \alpha \cdot (\vec{v_1}|\ldots|\vec{v_n})$. The components of $\alpha = (\vec{v_1}|\ldots|\vec{v_n})^{-1} \cdot \vec{u}$ are not necessarily integers (they are if $\Delta = |\det(\vec{v_1}|\ldots|\vec{v_n})| = 1$). However, $\Delta(\vec{v_1}|\ldots|\vec{v_n})^{-1}$ has integral coefficients hence $\Delta \vec{u}$ can be uniquely represented as an integral combination of the vectors $\vec{v_i}$: $\Delta \vec{u} = \Delta(\vec{v_1}|\ldots|\vec{v_n}) \cdot \alpha$, so there is a path to $O + \Delta \vec{u}$ whose length is: $\Delta(w_1 \ldots w_n) \cdot \alpha = \Delta(w_1 \ldots w_n) \cdot (\vec{v_1}|\ldots|\vec{v_n})^{-1} \cdot \vec{u} = \Delta \vec{\mathscr{F}} \cdot p \geqslant d(O, \Delta \vec{u})$. Thus $d(O, O + \Delta \vec{u}) < \Delta d(O, O + \vec{u})$ and the distance is not homogenous in the cone. $\square$

According to this proposition, the homogeneity in an nD unimodular cone can be determined by only testing the vectors of the cone (which are not necessarily in the chamfer mask). We derive a

necessary and sufficient condition for norms (a sufficient condition, based on a unimodular triangulation, is given in [10]):

Corollary 1 (*Norm condition*). *Let $\{U_i\}$ be a set of vectors sets U_i with the following properties*:

- *each unimodular cone $C_i = C_{O,U_i}$ intersects a unique facet of B_R;*
- *the union of the cones covers the entire space $\mathbb{Z}^n$.*

The chamfer mask $\mathscr{M}$ induces a norm if and only if:

$$d(O, O + \vec{u}) = \vec{\mathscr{F}} \cdot \vec{u}, \quad \forall \vec{u} \in \bigcup_i U_i. \tag{19}$$

Proposition 4 (*Direct distance formulation*). *If d induces a norm, the distance from O to any point p is*

$$d(O, p) = \max_{1 \leqslant i \leqslant l} \{\vec{\mathscr{F}}_i \cdot p\}, \tag{20}$$

where l is the number of facets of B_R and $\vec{\mathscr{F}}_i$ is the normal vector to the ith facet of B_R. This formula does not require to determine in which cone lies p.

Proof. The inequality $d(O, p) \geqslant \vec{\mathscr{F}}_i \cdot p$ holds for all facets due to Proposition 2 and the equality $d(O, p) = \vec{\mathscr{F}}_i \cdot p$ holds, according to Proposition 3, for all the facets of B_R (there is at least one of them) that intersect $[O, p)$. $\square$

3.4. $\mathscr{H}$-representation of chamfer norm balls

The $\mathscr{H}$-representation of chamfer balls is directly derived from (20):

$$p \in B_{\leqslant}(O, r) \quad \Leftrightarrow \quad \max_{1 \leqslant i \leqslant l} \{\vec{\mathscr{F}}_i \cdot p\} \leqslant r \quad \Leftrightarrow \quad A_{\mathscr{M}} \cdot p \leqslant y, \tag{21}$$

where $A_{\mathscr{M}}$ is an $\mathscr{H}$-representation matrix depending only on the chamfer mask $\mathscr{M}$. The number of rows in $A_{\mathscr{M}}$ is equal to the number l of facets of B_R, each line of the matrix $A_{\mathscr{M}}$ is computed with (16) and y is a column vector whose values are r. For instance, the $\mathscr{H}$-representation matrix of $d_{5,7,11}$ balls restricted to $\mathscr{G}$ is $A_{\mathscr{M}} = \begin{pmatrix} 5 & 1 \\ 4 & 3 \end{pmatrix}$ where $(5\ 1)$ and $(4\ 3)$ are the normal vectors of the two facets of B_R and $B_{\leqslant}(O, r) = \{p \in \mathbb{Z}^n : \begin{pmatrix} 5 & 1 \\ 4 & 3 \end{pmatrix} \cdot p \leqslant \begin{pmatrix} r \\ r \end{pmatrix}\}$.

Note that if a polytope is not centered in O, the simplification due to symmetries do not hold and the full set of $\mathscr{H}$-coefficients is needed, unless we ensure that the $\mathscr{H}$-coefficients for the hyperplanes in the generator $\mathscr{G}$ are greater than $\mathscr{H}$-coefficients for the corresponding symmetric cones. This is the case when a G-symmetric polytope is translated by a vector in $\mathscr{G}$.

Proposition 5 (*Furthest point*). *Let $A_{\mathscr{M}}$ be the matrix defined by a chamfer mask $\mathscr{M}$ generating a norm. The furthest point from the origin in the $\widehat{\mathscr{H}}$-polytope $P = \{p : A_{\mathscr{M}} \cdot p \leqslant \widehat{\mathscr{H}}(P)\}$ is at a distance equal to the greatest component of $\widehat{\mathscr{H}}(P)$.*

Proof. By construction of $A_{\mathscr{M}}$, (20) is equivalent to $d(O, p) = \max_i\{A_{\mathscr{M}i} \cdot p\}$, thus

$$\max_{p \in P}\{d(O, p)\} = \max_{p \in P}\left\{ \max_{1 \leqslant i \leqslant l} \{A_{\mathscr{M}i} \cdot p\} \right\} = \max_{1 \leqslant i \leqslant l} \{\widehat{\mathscr{H}}_i(P)\}. \quad \square$$

Proposition 6 (*Minimal covering ball*). *The radius of the minimal ball centered in O that contains all points of a discrete $\widehat{\mathscr{H}}$-polytope P represented by the matrix $A_{\mathscr{M}}$ and the vector $\widehat{\mathscr{H}}(P)$ is equal to the greatest component of $\widehat{\mathscr{H}}(P)$.*

Proof. The smallest ball that covers the polytope P must contain its furthest point from the origin:

$$\min\{r \in \mathbb{N} : P \subseteq B_{\leqslant}(O,r)\} = \max_{p \in P}\{d(O,p)\} = \max_{1 \leqslant i \leqslant l}\{\widehat{\mathcal{H}}_i(P)\}. \quad \square$$

Definition 14 (*Covering function*). We call *covering function* of a set X of points of $\mathbb{Z}^n$ the function $\mathscr{C}_X$ which assigns to each point p of $\mathbb{Z}^n$, the radius of the minimal ball centered in p covering X:

$$\mathscr{C}_X : \mathbb{Z}^n \to \mathbb{N},$$
$$\mathscr{C}_X(p) = \min\{r : X \subseteq B_{\leqslant}(p,r)\}.$$

The covering function of the chamfer ball $B_{\leqslant}(O,r)$ at point p gives the radius of the minimal ball centered in p that contains $B_{\leqslant}(O,r)$ or, by central symmetry of the chamfer balls, to the radius of the minimal ball centered in O covering $B_{\leqslant}(p,r)$ and therefore it is the maximal component of the $\widehat{\mathcal{H}}$-representation of $B_{\leqslant}(p,r)$:

$$\mathscr{C}_{B_{\leqslant}(O,r)}(p) = \max\{\widehat{\mathcal{H}}(B_{\leqslant}(p,r)) = \max\{\widehat{\mathcal{H}}(B_{\leqslant}(O,r)) + A_{\mathcal{M}} \cdot p\}. \quad (22)$$

One can notice that the covering function of the zero radius disk is equal to the distance function, as is the distance transform of the complement of this disk:

$$\mathscr{C}_{B_{\leqslant}(0,0)}(p) = \mathrm{DT}_{\mathbb{Z}^n \backslash \{O\}}(p) = d(p,O) = d(O,p).$$

Definition 15 (*Covering cone*). A *covering cone* $C_{o,U}$ in the covering function $\mathscr{C}_X$ is a unimodular cone defined by a vertex o and a set of vectors U, such that each ball centered in p is included in the ball centered in $p + \overrightarrow{u}$, $\overrightarrow{u} \in U$:

$$\forall p \in C_{o,U}, \ \forall \overrightarrow{u} \in U, \quad B_{\leqslant}(p, \mathscr{C}_X(p)) \subsetneq B_{\leqslant}(p + \overrightarrow{u}, \mathscr{C}_X(p + \overrightarrow{u})).$$

Proposition 7. *If $C_{o,U}$ is a covering cone in $\mathscr{C}_{B_{\leqslant}(O,r)}$ then for any point q in $C_{o,U} \backslash U \backslash \{o\}$ there exists p such that the ball centered in q includes the ball centered in p:*

$$B_{\leqslant}(O,r) \subsetneq B_{\leqslant}(p, \mathscr{C}_{B_{\leqslant}(O,r)}(p)) \subsetneq B_{\leqslant}(q, \mathscr{C}_{B_{\leqslant}(O,r)}(q)).$$

Proof. If U is not empty, there is $\overrightarrow{u} \in U$ such that $p = q - \overrightarrow{u}$ is in $C_{o,U} \backslash \{o\}$. Then, by definition of $C_{o,U}$, $B_{\leqslant}(p, \mathscr{C}_{B_{\leqslant}(O,r)}(p)) \subsetneq B_{\leqslant}(q, \mathscr{C}_{B_{\leqslant}(O,r)}(q))$. In addition, $B_{\leqslant}(O,r) \subseteq B_{\leqslant}(p, \mathscr{C}_{B_{\leqslant}(O,r)}(p))$ always holds by definition of $\mathscr{C}_{B_{\leqslant}(O,r)}$. $\quad \square$

Proposition 7 is used to limit the search for balls directly covering $B_{\leqslant}(O,r)$ in the covering function $\mathscr{C}_{B_{\leqslant}(O,r)}$. When a covering cone is detected, only its vertex o or the vectors of the cone (if $o = O$) have to be tested.

Proposition 8. *If there is an integer $j \in [1 \ldots l]$ and a point o such that $A_{\mathcal{M}j} \cdot \overrightarrow{u_i}$, $\forall \overrightarrow{u_i} \in U$ and $\widehat{\mathcal{H}}_j(B_{\leqslant}(o,r))$ are maximal then $C_{o,U}$ is a covering cone in $\mathscr{C}_{B_{\leqslant}(O,r)}$.*

Proof. Let j be the row number of a maximal component of $\widehat{\mathcal{H}}(B_{\leqslant}(o,r))$ and $A_{\mathcal{M}} \cdot \overrightarrow{u_i}$, $\forall \overrightarrow{u_i} \in U$, then j is a maximal component of any positive linear combination of these vectors. Let p be any point in $C_{o,U}$, $p = o + \sum_i \lambda_i \overrightarrow{u_i}$, $\lambda_i \in \mathbb{N}$. From (22), we deduce that, in $C_{o,U}$, $\mathscr{C}_{B_{\leqslant}(O,r)}$ takes the form of an affine function of the components λ_i:

$$\mathscr{C}_{B_{\leqslant}(O,r)}(p) = \max\left\{\widehat{\mathcal{H}}(B_{\leqslant}(o,r)) + \sum \lambda_i A_{\mathcal{M}} \overrightarrow{u_i}\right\}$$
$$= \widehat{\mathcal{H}}_j(B_{\leqslant}(o,r)) + \sum \lambda_i A_{\mathcal{M}j} \overrightarrow{u_i}.$$

In the same way, the radius of the minimal ball centered in $p + \overrightarrow{u}$, $\overrightarrow{u} \in U$ covering $B_{\leqslant}(O,r)$ is

$$\mathscr{C}_{B_{\leqslant}(O,r)}(p + \overrightarrow{u}) = \widehat{\mathcal{H}}_j(B_{\leqslant}(o,r)) + \sum \lambda_i A_{\mathcal{M}j} \overrightarrow{u_i} + A_{\mathcal{M}j} \overrightarrow{u}$$
$$= \mathscr{C}_{B_{\leqslant}(p, \mathscr{C}_{B_{\leqslant}(O,r)}(p))}(O + \overrightarrow{u}).$$

In other words, $B_{\leqslant}(p, \mathscr{C}_{B_{\leqslant}(O,r)}(p))$ is contained in $B_{\leqslant}(p + \overrightarrow{u}, \mathscr{C}_{B_{\leqslant}(O,r)}(p + \overrightarrow{u}))$ and $C_{o,U}$ is a covering cone according to Definition 15. $\quad \square$

4. Triangulation of 3D chamfer balls

The first stage of the method consists in decomposing the generator cone $\mathcal{G}$ in unimodular cones that each intercepts a unique facet of the rational ball. This triangulation has three goals:

1. compute the distance gradients which are vectors normal to the facets of the rational ball. These distance gradients are the rows of the matrix $A_{\mathcal{M}}$;
2. provide a set of unimodular cones suitable for the recursive partition of the generator $\mathcal{G}$ used in the next stage;
3. verify that the chamfer mask generates a norm by checking homogeneity in each cone.

4.1. Convex hull vertices in the generator cone

The expected result is a triangulation of the part of the rational ball B_R that lies in the generator $\mathcal{G}$. The input data consist of vectors from the chamfer mask $\mathcal{M}|_{\mathcal{G}}$ divided by their corresponding weights (to form the equivalent unitary ball). In the algorithm, these points in $\mathbb{Q}^n$ are represented as weightings, and all computations are based on integer arithmetics. The weightings of the chamfer mask are not sufficient alone because

$$\mathcal{G} \cap \mathrm{conv}\left(\frac{\overrightarrow{v}}{w}, (\overrightarrow{v};w) \in \mathcal{M}\right) \neq \mathrm{conv}\left(\frac{\overrightarrow{v}}{w}, (\overrightarrow{v};w) \in \mathcal{M}|_{\mathcal{G}}\right).$$

The intersection of B_R with $\mathcal{G}$ introduces new vertices that are points in edges of B_R that intersect the faces of $\mathcal{G}$. This is illustrated in Fig. 3(a); vectors $\overrightarrow{e} = (2\ 1\ 1)$ and $\overrightarrow{o} = (4\ 1\ 1)$ are not in the chamfer mask and thus cannot be vertices of B_R, but they appear in the intersection of B_R with $(O, \{\overrightarrow{a}, \overrightarrow{c}\})$. Since the edges of B_R are not known yet, all the intersections of the faces of $\mathcal{G}$ with couples of rational vertices of B_R must be added to the input of the algorithm. These points are rational combinations of the vertices of the intersected edges, but are also represented as weightings with integer coefficients. Among those, the majority of the points that lie in the interior of B_R will be discarded during the computation of the convex hull.

4.2. Gift-wrapping convex hull and triangulation of the rational ball

Many different algorithms are available for convex hull computation. We chose to implement an modified version of the algorithm known as *gift wrapping* [20] for two reasons: first, it naturally produces a triangulation of the convex hull i.e. a partition in simplicial cones and second, a subpartition of these simplicial cones in unimodular cones and the face lattice of the cones can be easily integrated as by-products of the algorithm.
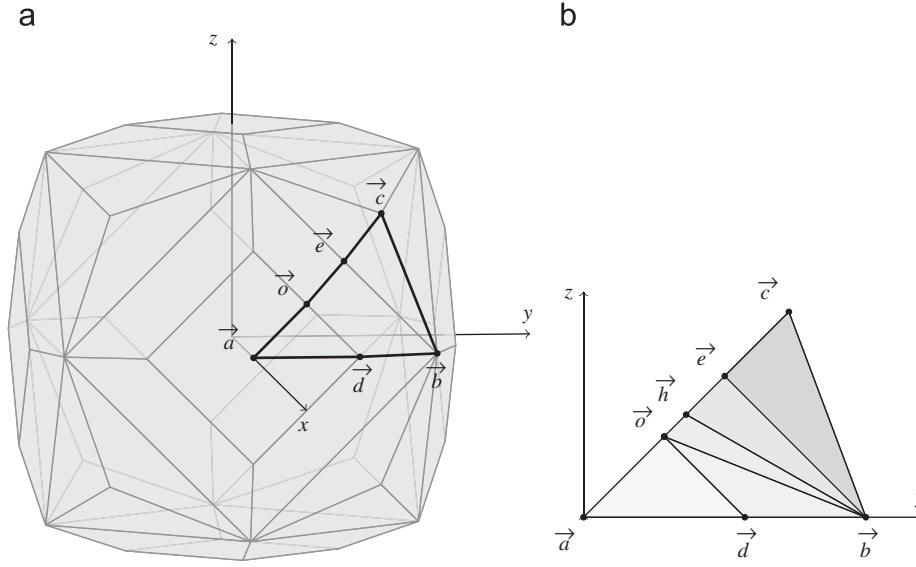
a

b

Fig. 3. The rational ball B_R of the 3D chamfer mask $7, 8, 11, 14$ and a unimodular triangulation of $B_R \cap \mathcal{G}$. Unimodular triangulation in 3D cones (represented by triangles) of $B_R \cap \mathcal{G}$ (thick lines in (a)). Each $\mathbb{Z}^3$ point (x, y, z) is projected onto $(y/x, z/x)$ (Farey space).

Algorithm 1. (Simplified) gift wrapping algorithm [20].

    Input: A set of points S
1 find a starting edge of the convex hull (p, q)
2 push (p, q) in ℓ, the list of active edges
3 **while** L is not empty **do**
4   pop (p, q) from ℓ
5   take r in $S \backslash \{p, q\}$
6 $S' \leftarrow S \backslash \{p, q, r\}$
7   **for** s in S' **do**
8   **if** s is above (p, q, r) **then**
9 $r \leftarrow s$
10   **end**
11   **end**
12   add each newly created edge (r, p) and (q, r) in ℓ or remove
       it from ℓ if already contained
13 end

Starting with a first edge, the *gift wrapping* algorithm 1 iteratively extends the convex hull by appending a new triangle and its edges. Since the convex hull is computed in $\mathcal{G}$, one vertex of the starting edge can be chosen as the point in the first axis of $\mathcal{G}$ that is closest to the origin: $p = (x_1, 0, 0)$ (with maximal x_1 if several points exist on this axis) and the second vertex is the point q that maximizes the angle (O, p, q) in a facet of $\mathcal{G}$ containing p. The algorithm proceeds until exhaustion of active edges.

4.3. Unimodular triangulation

The *gift wrapping* algorithm produces a set of nD simplicial cones $C_{o,U}$, each of which is unimodular if and only if $\det(U) = \pm 1$. When $|\det(U)| > 1$, a new point is introduced as an input of the convex hull computation and the detected non-unimodular cone is discarded. The unimodular triangulation is represented by a cone lattice $\mathcal{L}$ used later as a partition of $\mathcal{G}$.

The intersection of the rational ball for mask $7, 8, 11, 14$ and $\mathcal{G}$ is pictured in Fig. 3(b). A unimodular triangulation without any new point of the face ($\vec{b} = (1\ 1\ 0)$, $\vec{d} = (2\ 1\ 0)$, $\vec{e} = (2\ 1\ 1)$, $\vec{o} = (4\ 1\ 1)$) cannot be made because $\det(\vec{d}, \vec{e}, \vec{o}) = \det(\vec{b}, \vec{e}, \vec{o}) = 2$. This is

solved by introducing the vector $\vec{h}$. The cone lattice corresponding to this unimodular triangulation is pictured in Fig. 4.

4.4. Homogeneity check

The unimodular triangulation of B_R produces a set of cones that cover the generator $\mathcal{G}$ and their corresponding face normal vectors. Using Corollary 1, by comparing $d(O, O + \vec{u})$, obtained by propagating the chamfer weights, with $\vec{\mathcal{F}}_i \cdot \vec{u}$, where $\vec{\mathcal{F}}$ is the normal vector of one of the faces that intersects $[O, \vec{u})$, we determine if the distance is homogenous in $\mathcal{G}$, so by symmetry, in $\mathbb{Z}^3$.

5. LUT and test neighborhood computation for 3D chamfer norms

5.1. $\widehat{\mathcal{H}}$-representation of chamfer balls

The computation of the LUT is based on an $\widehat{\mathcal{H}}$-representation of the chamfer norm balls. All share the same matrix $A_{\mathcal{M}}$ which depends only on the chamfer mask (21). The $\widehat{\mathcal{H}}$-coefficients of the balls are computed iteratively from the ball of radius 0, $B_{\leqslant}(O, 0) = \{x : A_{\mathcal{M}}x = 0\}$ using (14) and (11):

$$\widehat{\mathcal{H}}(B_{\leqslant}(O, r)) = \max\{\widehat{\mathcal{H}}(B_{\leqslant}(O, r-1)); \widehat{\mathcal{H}}(B_{\leqslant}(O, r - w_i)) + A_{\mathcal{M}} \vec{v}_i,$$
$$i \in [1 \dots m]\}.$$

5.2. LUT values

LUT values are directly obtained from the covering function (22):

$$\text{Lut}_{\vec{v}_i}[r] = 1 + \mathscr{C}_{B_{\leqslant}(O, r-1)}(O + \vec{v}_i)$$
$$= 1 + \max\{\widehat{\mathcal{H}}(B_{\leqslant}(O, r-1)) + A_{\mathcal{M}} \cdot \vec{v}_i\}.$$

5.3. Test neighborhood

Algorithm 2 begins with an empty test neighborhood $\mathcal{T}$ and seek direct covering relations in balls of increasing radii like the method
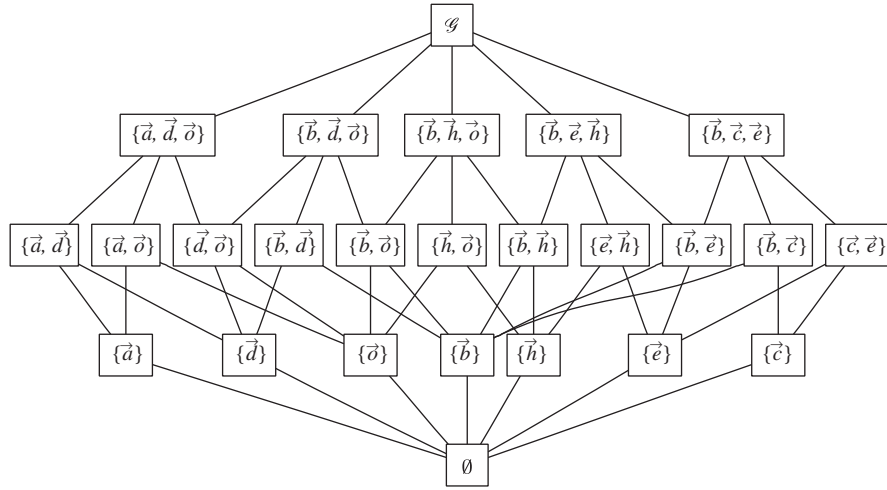
Fig. 4. Lattice of cone vector sets for the unimodular triangulation of $B_R \cap \mathscr{G}$ (chamfer mask $7, 8, 11, 14$).
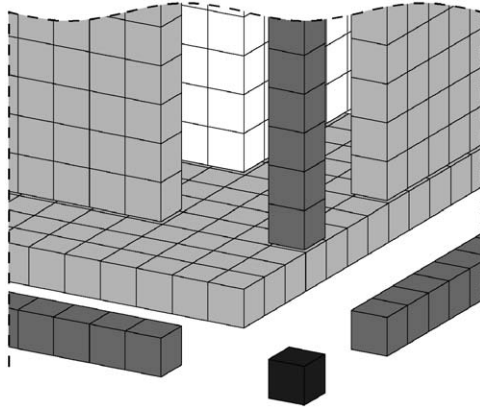

Fig. 5. The partition of a 3D unimodular cone in 2^3 subcones (from darkest to lightest): 1 point, $C_1^3 = 3$ 1D cones, $C_2^3 = 3$ 2D cones and $C_3^3 = 1$ 3D cone.

in [7]. However, in [7], the covering relations are seen from the perspective of the covering balls (in the distance map, requiring propagation of distances), whereas in our case, they are considered from the point of view of the covered balls, i.e. in the covering function that can be computed directly without propagation using the direct formula (22). The algorithm uses the lattice of cones $\mathscr{L}$ (Fig. 4), resulting from the triangulation phase, as a partition of $\mathscr{G}$. Each cone that is not a covering cone is recursively partitioned by procedure visitCone as depicted in Fig. 5: a nD cone $C_{o,U}$ is divided into 2^n subcones corresponding to all the subsets of U. Direct covering relations at the vertices of all the visited cones are checked by procedure visitPoint using a direct computation of the covering function in all known neighbors in $\mathscr{T}$.

Algorithm 2. Computation of the test neighborhood.

Input: $\mathscr{L}$ lattice of simplicial unimodular cones, maximal radius R
1 $\mathscr{T} \leftarrow \emptyset$
2 **for** $r \leftarrow 1$ **to** R **do**   // inner radius
3   **foreach** $C_{O,U} \in \mathscr{L}$ **do**   // cones with increasing dimension
4       $o \leftarrow O + \sum_{\overrightarrow{u} \in U} \overrightarrow{u}$;
5   visitCone$(\mathscr{T}, C_{o,U}, r)$;
6   **end**
7 **end**

6. Results

An implementation of these algorithms was developed in the C language. It produces output in the same format as the reference algorithm [7] so that outputs can be compared character-to-character. Tests were done on various chamfer masks and different maximal radii and helped discover a propagation issue in the reference algorithm. This problem corrected, the results are almost always identical except for insignificant cases close to the maximal radius for which covering radii exceed the maximum. These radii are handled differently by both algorithms but since they exceed the maximum radius, there is no impact on the medial axis computation.

Procedure. visitCone$(\mathscr{T}, C_{o,U}, r)$.

Input: $\mathscr{T}$, $C_{o,U}$, inner radius r, $y = \widehat{\mathscr{H}}(B_{\leqslant}(o, r))$
1 visitPoint(o)
  // Visit subcones if $C_{o,U}$ is not a covering cone
2 **if** $\forall j, \forall \overrightarrow{u} \in U : y_j \neq \max_k\{y_k\}$ *and* $A_{\mathscr{M}j} \cdot \overrightarrow{u} \neq \max_k\{A_{\mathscr{M}k} \cdot \overrightarrow{u}\}$ **then**
3   **foreach** *subcone* $C_{o,U'}$ *of* $C_{o,U}$ **do**
4       $o' \leftarrow o + \sum_{\overrightarrow{u} \in U'} \overrightarrow{u}$;
5   visitCone$(\mathscr{T}, C_{o',U'}, r)$;
6   **end**
7 **end**

Procedure. visitPoint$(\mathscr{T}, r, p)$.

Input: $\mathscr{T}$, inner radius r, ball center p to test
1 **if** $\forall \overrightarrow{v} \in \mathscr{T} : B_{\leqslant}(O + \overrightarrow{v}, \mathscr{C}_{B_{\leqslant}(O,r)}(O + \overrightarrow{v})) \not\sqsubset B_{\leqslant}(p, \mathscr{C}_{B_{\leqslant}(O,r)}(p))$ **then**
2    $\mathscr{T} \leftarrow \mathscr{T} \cup \{\overrightarrow{Op}\}$
3 **end**

The run times of both reference and proposed algorithms are given in Table 1 for various sizes and a few masks. These figures show that the overall mean computational complexity is linear with the maximal radius for the proposed method, whereas it is of order r^4 in 3D for the reference algorithm.

7. Conclusion

In this paper, methods to compute both the chamfer LUT and the test neighborhood were presented. Speed gains from the reference algorithm [7] are attributable to the representation of chamfer balls as $\mathscr{H}$-polytopes. With this description, we avoid the use of weight

Table 1
Run times (in seconds) of reference (ref.) and proposed ($\mathscr{H}$) method implementations for four 3D masks and various volume sizes $L \times L \times L$.

L	3, 4, 5		3, 4, 5, 7		7, 8, 11, 14		4, 6, 7, 9, 10	
	Ref.	$\mathscr{H}$	Ref.	$\mathscr{H}$	Ref.	$\mathscr{H}$	Ref.	$\mathscr{H}$
10	0.0006	0.0003	0.0002	0.0004	0.0013	0.0010	0.0004	0.0008
20	0.0049	0.0002	0.0032	0.0004	0.0135	0.0011	0.0047	0.0010
50	0.1079	0.0003	0.1096	0.0005	0.2886	0.0027	0.1592	0.0015
100	1.6316	0.0005	1.6831	0.0008	4.4704	0.0054	2.4626	0.0023
200	30.391	0.0010	31.126	0.0012	81.627	0.0109	53.126	0.0038
500	3523	0.0022	3537	0.0024	9333	0.0272	6465	0.0088
1000		0.0042		0.0073		0.0549		0.0220

propagation in the image domain and obtain a constant time covering test by the direct computation of covering radii. Moreover the search space is greatly reduced using covering cones.

While applications always using the same mask can use precomputed test neighborhood $\mathscr{T}$ and LUT, other applications that potentially use several masks, adaptive masks, variable input image size can benefit from these algorithms. A faster computation of $\mathscr{T}$ is also highly interesting to explore chamfer mask properties. Beyond improved run times, the $\mathscr{H}$-polytope representation helped to prove new properties of chamfer masks. And a new formula of distance which does not need to find in which cone lies a point was given.

Examples and source codes for the 3D and 2D cases are available by simple email request to the authors or in the code section of the IAPR-TC18 web site (http://www.cb.uu.se/~tc18/).

Acknowledgment

References

[1] A. Rosenfeld, J.L. Pfaltz, Sequential operations in digital picture processing, Journal of the ACM 13 (4) (1966) 471–494.
[2] U. Montanari, A method for obtaining skeletons using a quasi-Euclidean distance, Journal of the ACM 15 (4) (1968) 600–624.
[3] G. Borgefors, Distance transformations in arbitrary dimensions, Computer Vision, Graphics, and Image Processing 27 (3) (1984) 321–345.
[4] D. Coeurjolly, A. Montanvert, Optimal separable algorithms to compute the reverse Euclidean distance transformation and discrete medial axis in arbitrary dimension, IEEE Transactions on Pattern Analysis and Machine Intelligence 29 (3) (2007) 437–448.
[5] R. Strand, Weighted distances based on neighborhood sequences, Pattern Recognition Letters 28 (15) (2007) 2029–2036.
[6] G. Borgefors, Centres of maximal discs in the 5–7–11 distance transforms, in: Proceedings of the 8th Scandinavian Conference on Image Analysis, Tromso, Norway, 1993, pp. 105–111.
[7] É. Rémy, É. Thiel, Medial axis for chamfer distances: computing look-up tables and neighbourhoods in 2D or 3D, Pattern Recognition Letters 23 (6) (2002) 649–661.
[8] N. Normand, P. Évenou, Medial axis LUT computation for chamfer norms using $\mathscr{H}$-polytopes, in: Discrete Geometry for Computer Imagery, Lecture Notes in Computer Sciences, vol. 4992, Springer, Berlin, Heidelberg, 2008, pp. 189–200. doi: 10.1007/978-3-540-79126-3_18.
[9] A. Rosenfeld, J. Pfaltz, Distances functions on digital pictures, Pattern Recognition Letters 1 (1) (1968) 33–61.
[10] É. Thiel, Géométrie des distances de chanfrein, mémoire d'habilitation à diriger des recherches, Université de la Méditerranée, Aix-Marseille 2, December 2001 ⟨http://www.lif-sud.univ-mrs.fr/~thiel/hdr/⟩.
[11] B.J.H. Verwer, Local distances for distance transformations in two and three dimensions, Pattern Recognition Letters 12 (11) (1991) 671–682.
[12] É. Rémy, Normes de chanfrein et axe médian dans le volume discret, Thèse de doctorat, Université de la Méditerranée, December 2001.
[13] C. Arcelli, G. Sanniti di Baja, Finding local maxima in a pseudo-Euclidian distance transform, Computer Vision, Graphics, and Image Processing 43 (3) (1988) 361–367.
[14] S. Svensson, G. Borgefors, Digital distance transforms in 3D images using information from neighbourhoods up to $5 \times 5 \times 5$, Computer Vision and Image Understanding 88 (1) (2002) 24–53.
[15] É. Thiel, Les distances de chanfrein en analyse d'images: fondements et applications, Thèse de doctorat, Université Joseph Fourier, Grenoble 1, September 1994 ⟨http://www.lif-sud.univ-mrs.fr/~thiel/these/⟩.
[16] É. Rémy, É. Thiel, Computing 3D medial axis for chamfer distances, in: Discrete Geometry for Computer Imagery, Uppsala, Sweden, Lecture Notes in Computer Science, vol. 1953, Springer, Berlin, 2000, pp. 418–430. doi: 10.1007/3-540-44438-6_34.
[17] G.M. Ziegler, Lectures on Polytopes (Graduate Texts in Mathematics), Springer, Berlin, 2001.
[18] G. Borgefors, Weighted digital distance transforms in four dimensions, Discrete Applied Mathematics 125 (1) (2003) 161–176.
[19] C. Fouard, G. Malandain, 3-D chamfer distances and norms in anisotropic grids, Image and Vision Computing 23 (2) (2004) 143–158.
[20] D.R. Chand, S.S. Kapur, An algorithm for convex polytopes, Journal of the Association for Computing Machinery 17 (1) (1970) 78–86.

About the Author—NICOLAS NORMAND was born in 1969. He received the M.S. degree in 1992 and his Ph.D. from the University of Nantes, France, in 1997. He has been an assistant professor in the Computer Science Department of École Polytechnique de l'Université de Nantes from 1997. His areas of interest include digital geometry and particularly discrete distances, data networks and the related Mojette transform.

About the Author—PIERRE EVENOU was born in 1973. He received the M.S. degree in 2003. He has been an research engineer in the Computer Science Department of École Polytechnique de l'Université de Nantes from 2005. His areas of interest include digital geometry and particularly discrete distances, data networks and the related Mojette transform.